

^{40}Ca transverse response function from coupled-cluster theory

J. E. Sobczyk,¹ B. Acharya,^{2,1} S. Bacca,^{1,3} and G. Hagen^{2,4}

¹*Institut für Kernphysik and PRISMA⁺ Cluster of Excellence,
Johannes Gutenberg-Universität, 55128 Mainz, Germany*

²*Physics Division, Oak Ridge National Laboratory, Oak Ridge, TN 37831, USA*

³*Helmholtz-Institut Mainz, Johannes Gutenberg-Universität Mainz, D-55099 Mainz, Germany*

⁴*Department of Physics and Astronomy, University of Tennessee, Knoxville, TN 37996, USA*

We present calculations of the ^{40}Ca transverse response function obtained from coupled-cluster theory used in conjunction with the Lorentz integral transform method. We employ nuclear forces derived at next-to-next-to leading order in chiral effective field theory with and without Δ degrees of freedom. We first benchmark this approach on the ^4He nucleus and compare both the transverse sum rule and the response function to earlier calculations based on different methods. As expected from the power counting of the chiral expansion of electromagnetic currents and from previous studies, our results retaining only one-body term underestimate the experimental data for ^4He by about 20%. However, when the method is applied to ^{40}Ca at the same order of the expansion, response functions do not lack strength and agree well with the world electron scattering data. We discuss various sources of theoretical uncertainties and comment on the comparison of our results with the available experiments.

I. INTRODUCTION

A longstanding quest in nuclear physics is to accurately describe a wide range of nuclear phenomena by treating nuclei as systems of protons and neutrons interacting among themselves and with external fields. In a so-called “*ab initio*” approach, the nuclear many-body Schrödinger equation is solved, either exactly or using controlled approximations, by employing nuclear forces that are constrained by the symmetries of quantum chromodynamics, nucleon-nucleon (NN) scattering experiments, and selected nuclear data [1, 2]. Modern *ab initio* computations have increasingly adopted chiral effective field theory (χEFT) to derive nuclear forces, providing a rigorous framework to organize NN, three-nucleon (3N) and many-nucleon forces, as well as currents that couple nucleons to external fields, into a low-momentum expansion [3]. The close relation between the nuclear Hamiltonians and electroweak currents makes χEFT studies of electroweak observables very interesting [4, 5]. Extending *ab initio* studies to electroweak cross sections is important to test the theory, to estimate theoretical uncertainties, and to possibly improve on the precision.

Traditionally applied to light and closed-shell medium-mass nuclei, *ab initio* methods have recently found success in describing heavy [6], deformed [7–13], and exotic [14, 15] nuclei. Coupled-cluster theory [16–25] played an important role in these achievements among other computational methods that exhibit a polynomial scaling with the number of nucleons (see Ref. [1] for a recent review). Extensions of *ab initio* studies to processes that involve nuclear excitations in the continuum is an important frontier [26]. Recently, the Lorentz integral transform method [27] was reformulated within coupled-cluster theory to generate an approach called LIT-CC which is well suited to study nuclear responses induced by electroweak probes. Within this approach, the sum over continuous final states is reformulated in terms of

an integral transform and later inverted to access the response function. The LIT-CC method was extensively benchmarked on electric dipole excitations of medium-mass nuclei [28–30], but it can be extended to a variety of electroweak observables.

In addition to improving our understanding of the nuclear dynamics, one of the main motivations to investigate electroweak response functions is the neutrino experiments, especially the long-baseline programs, which require reliable predictions of neutrino-nucleus cross-sections to perform the neutrino energy reconstruction and, from there, infer the oscillations parameters. The quasi-elastic peak is the dominating mechanism in the T2K and the future HyperK [31] experiments, and is also an important reaction channel for DUNE [32]. Presently, the only *ab initio* predictions of neutrino cross sections in this region are available from the Green’s Function Monte Carlo (GFMC) method for light nuclei up to ^{12}C [33–36]. Under certain approximations, other methods, such as the short-time approximation [37] or the spectral function [38–40], have been proposed to connect the cross sections with *ab initio* calculations. Recently there has also been progress in computing the ^{16}O spectral function calculated within coupled-cluster theory [41].

In this endeavor, electron-scattering experiments play an important role in guiding theoretical studies [42]. Due to an analogous structure of electron- and neutrino-nucleus cross-sections, the precise electron data provide a stringent test for our modeling of the nuclear dynamics. The Rosenbluth technique allows a separation of the electron-scattering cross section into the longitudinal and the transverse response functions, which are driven by the electric charge and the electromagnetic current operators, respectively. Using the LIT-CC approach, we successfully described the longitudinal response function at the momentum transfers of a few hundred MeV in the region medium-mass nuclei [40, 43]. The final state interactions were consistently taken into account, leading to

a very good agreement with available experimental data on ${}^4\text{He}$ and ${}^{40}\text{Ca}$.

In this work, we further extend the LIT-CC method to describe the transverse response function, which dominates the cross section at backward scattering angles. We provide the first *ab initio* results for mass number $A = 40$ in the impulse approximation. This is an important step towards building a complete and systematic theory for lepton-nucleus scattering.

The article is structured as follows. In Sec. II, we introduce the definition of the transverse response function and describe the framework in which we perform calculations. We present our results in Sec. III, starting from the transverse sum rule for ${}^4\text{He}$ and ${}^{40}\text{Ca}$ and benchmark with existing calculations. Next, we present the response functions for these two nuclei up to 400 MeV/c, commenting on the tensions existing in available experimental data on ${}^{40}\text{Ca}$. Finally, we conclude in Sec. IV.

II. FORMALISM

The inclusive electron-nucleus scattering cross-section in the Born approximation can be expressed in terms of longitudinal and transverse response functions. The focus of this work is the transverse response function R_T , which depends on the energy and momentum transfer (ω, q) , and is defined as

$$R_T(\omega, q) = \sum_f |\langle \Psi_f | \mathbf{J}^T(q) | \Psi_0 \rangle|^2 \delta(E_f + \frac{q^2}{2M} - E_0 - \omega). \quad (1)$$

Here, \mathbf{J}^T corresponds to the transverse part of the electromagnetic current operator with respect to the direction of the vector momentum transfer \mathbf{q} . In Eq. (1), the nuclear ground state wavefunction is denoted by Ψ_0 (with corresponding energy E_0) and we sum over all possible final states Ψ_f (with energy E_f) which obey the energy conservation expressed by the delta function, where M is the mass of the nucleus and $q = |\mathbf{q}|$.

In the impulse approximation, the current operator can be decomposed into the isoscalar and isovector parts $\mathbf{J} = \mathbf{J}_s + \mathbf{J}_v$, as

$$\begin{aligned} \mathbf{J}_s &= \sum_{j=1}^A \left(G_E^S(Q^2) \frac{\mathbf{p}_j}{m} - i G_M^S(Q^2) \frac{\mathbf{q} \times \boldsymbol{\sigma}_j}{2m} \right) e^{i\mathbf{q} \cdot \mathbf{r}_j} \frac{1}{2}, \\ \mathbf{J}_v &= \sum_{j=1}^A \left(G_E^V(Q^2) \frac{\mathbf{p}_j}{m} - i G_M^V(Q^2) \frac{\mathbf{q} \times \boldsymbol{\sigma}_j}{2m} \right) e^{i\mathbf{q} \cdot \mathbf{r}_j} \frac{\tau_j^z}{2}. \end{aligned} \quad (2)$$

Here, one can clearly identify the convection and spin terms, which depend on the nucleon momenta \mathbf{p}_j and spins $\boldsymbol{\sigma}_j$, respectively. The nucleon mass is indicated with m and its third isospin component with τ_j^z , while $G_{E,M}^S \equiv G_{E,M}^p + G_{E,M}^n$, $G_{E,M}^V \equiv G_{E,M}^p - G_{E,M}^n$ are the electric and magnetic form factors related to the proton

and neutron form factors. They are functions of $Q^2 = q^2 - \omega^2$. However, in our calculation the dependence on the energy transfer ω is not known *a priori*, so we assume $\omega \approx \sqrt{q^2 + m^2} - m$ which corresponds to the kinematical region of the quasi-elastic peak. This approximation has been previously applied in GFMC calculations [36, 44]. While several parameterizations exist for the form factor, in our calculations we use that from Ref. [45].

The transverse response function is known to receive a large contribution from two-nucleon currents which are required by the continuity equation [5]. This fact has been confirmed by Green function Monte Carlo calculations for light nuclei up to ${}^{12}\text{C}$ using phenomenological potentials and currents [36]. It is also expected from the power counting when performing the chiral expansion of electromagnetic currents, where the two-body currents appear at the same order as the leading one-body currents in the counting advocated by Refs. [46, 47] and are suppressed by only one chiral order in the power counting adopted by Refs. [48, 49]. In this work we only include the one-body current contributions as a first step. The study of the role of two-body currents is left for future work.

A. Lorentz integral transform

The sum over continuum spectrum of final states in Eq. (1) poses a serious computational challenge. To overcome it, we follow the Lorentz integral transform method [50]. First, we calculate the convolution of the nuclear response function with the Lorentzian kernel

$$K(\omega, \sigma) = \frac{\sigma_I}{\pi} \frac{1}{(\omega - \sigma_R)^2 + \sigma_I^2} \quad (3)$$

as

$$\mathcal{L}_T(\sigma, q) = \int d\omega R_T(\omega, q) K(\omega, \sigma), \quad (4)$$

where $\sigma = \sigma_R + i\sigma_I$ is a complex parameter. Using Eqs. (1) and (4), $\mathcal{L}_T(\sigma, q)$ can be formally expressed as the solution of a ‘‘Schrödinger-like’’ equation with a source term

$$(H - E_0 - \sigma) |\tilde{\Psi}_\sigma(q)\rangle = \mathbf{J}^T(q) |\Psi_0\rangle. \quad (5)$$

The latter can be solved with a good many-body bound-state technique, so that the integral transform of the response function becomes

$$\mathcal{L}_T(\sigma, q) = \langle \tilde{\Psi}_\sigma(q) | \tilde{\Psi}_\sigma(q) \rangle \quad (6)$$

and can be numerically evaluated. The response $R_T(\omega, q)$ is then retrieved from $\mathcal{L}_T(\sigma, q)$ through an inversion procedure. In general, the inversion is an ill-posed problem which requires some additional assumptions about the shape of the response function [50]. We invert the transform assuming that the final response function is smooth. This assumption is fully justified in the region of the quasi-elastic peak.

B. Coupled-cluster method

In the coupled-cluster method many-body correlations are systematically included to the wave function through an exponential ansatz e^T acting on a reference state Φ_0 . The correlation operator T is a linear expansion in n -particle n -hole excitation operators with respect to the reference state,

$$T = T_1 + T_2 + \dots + T_A \quad (7)$$

The Schrödinger equation, rewritten with the coupled-cluster ansatz, becomes then

$$H_N e^T |\Phi_0\rangle = E_0 e^T |\Phi_0\rangle \quad \rightarrow \quad \bar{H}_N |\Phi_0\rangle = E_0 |\Phi_0\rangle, \quad (8)$$

where $\bar{H}_N \equiv e^{-T} H_N e^T$ is the similarity transformed normal ordered Hamiltonian, and Φ_0 is the Hartree-Fock solution to a Hamiltonian containing nucleon-nucleon and three-nucleon forces. The excitation operator T is usually truncated at some low excitation rank. In this work, we use $T \approx T_1 + T_2$, which is known as coupled-cluster with single and double excitations (CCSD) [51]. This approximation is known to account for $\sim 90\%$ of the correlation energy in the ground state for systems with a well defined Fermi surface [52].

C. The LIT-CC method

The Lorentz integral transform method has been recently formulated within coupled-cluster theory [53]. In this language, Eq. (6) becomes

$$\begin{aligned} (\bar{H}_N - E_0 - \sigma) |\tilde{\Psi}_\sigma^R(q)\rangle &= \bar{\Theta}_J |\Phi_0\rangle, \\ \langle \tilde{\Psi}_\sigma^L(q) | (\bar{H}_N - E_0 - \sigma) &= \langle \Phi_0 | (1 + \Lambda) \bar{\Theta}_J, \end{aligned} \quad (9)$$

where $\bar{\Theta}_J \equiv e^{-T} \Theta_J e^T$ is a similarity transformed operator. Given that coupled-cluster theory is non-Hermitian, we solve both the left and right equations separately for $\tilde{\Psi}_\sigma^L(q)$ and $\tilde{\Psi}_\sigma^R(q)$ to get

$$\mathcal{L}_T(\sigma, q) = \langle \tilde{\Psi}_\sigma^L(q) | \tilde{\Psi}_\sigma^R(q) \rangle. \quad (10)$$

The operator $\Lambda = \Lambda_1 + \Lambda_2 + \dots$ is a de-excitation operator which has an analogous structure as T operator and accounts for the fact that the left and right eigenstates are not the same. The equations in (9) are both equations-of-motion with a source term. They can be solved, after having solved for the ground-state, using similar techniques to the standard ones to get the spectrum of excited states within coupled-cluster theory [53, 54].

The operator Θ_J is a multipole, i.e., a spherical rank- J tensor, of the transverse electromagnetic current, namely $\mathbf{J}^T(q) \equiv \sum_{J=0}^{J_{max}} \Theta_J$. Expressions for the multipoles of the current operators can be found in Ref. [55]. After calculating the LITs of Eq. (10) for each rank- J multipole, we sum them up, and finally perform an inversion of the total integral transform.

III. RESULTS

We now present results focusing on the nuclei ${}^4\text{He}$, which we will use as a benchmark, and ${}^{40}\text{Ca}$. All the results presented in this section are obtained within a model space of 15 major oscillator shells which proved to be sufficient for systems and observables we compute [43]. An additional cut is imposed on the three-body potential $e_{3\text{max}} = 2n_1 + l_1 + 2n_2 + l_2 + 2n_3 + l_3 \leq 16$. We check the convergence of the model space by varying the underlying harmonic oscillator frequency. We use two different chiral Hamiltonians at the next-to-next-to-leading order: NNLO_{sat} [56] and Δ NNLO_{GO}(450) [57]. In the latter one, the Δ degree of freedom is considered explicitly in the construction of nuclear potential. Both interactions have the same regulator cut-off of 450 MeV/c. They predict correct binding energies and radii for light and medium-mass nuclei, in particular the ones we consider.

A. Transverse sum rule

The transverse sum rule is defined in a standard way as

$$\text{TSR}(q) = \frac{2m^2}{Z\mu_p^2 + N\mu_n^2} \frac{1}{q^2} \left(\langle \Psi_0 | \mathbf{J}^{T\dagger} \mathbf{J}^T | \Psi_0 \rangle - |\langle \Psi_0 | \mathbf{J}^T | \Psi_0 \rangle|^2 \right). \quad (11)$$

with the nucleon magnetic moments $\mu_{n,p}$. The elastic contribution (second line) is zero for the closed-shell nuclei which we consider. The normalization is chosen in such a way that $\text{TSR}(q \rightarrow \infty) \approx 1$. We use this limit as a numerical check of the multipole decomposition of the current. Let us first benchmark our transverse sum rule result for ${}^4\text{He}$. We employed the NNLO_{sat} potential with the underlying harmonic oscillator frequency $\hbar\Omega = 16$ MeV, in accordance with our previous benchmarks of the longitudinal response and Coulomb sum rule [40].

As shown in Fig. 1, we obtain a very good agreement above $q = 200$ MeV/c when comparing with other simulations which use either AV14+UVII [58] or AV18+UIX potentials [59], for the variational Monte Carlo (VMC) and the correlated hyperspherical harmonics (CHH) methods, respectively. The low- q behavior diverges (because of the $1/q^2$ factor in the definition of the sum rule, see Eq. (11)) and differs quite substantially from the calculation of Ref. [58] that employed a phenomenological potential. In the limit of $q \rightarrow 0$, the spin part of the current becomes negligible, while the convection-current contribution becomes proportional to the kinetic energy (see Eq. (2)). The latter strongly depends on the employed Hamiltonian, which explains the difference between the calculations. We performed an internal check of our method, comparing our result with an average kinetic energy $\langle T \rangle = \int d^3p n(p) p^2 / 2m$ where $n(p)$ is the momentum distribution. We obtained agreement within a few percent.

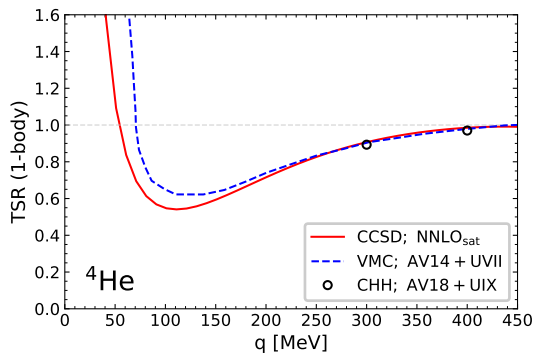


FIG. 1. ${}^4\text{He}$ results for transverse sum rule for $\text{N}^2\text{LO}_{\text{sat}}$ and $\hbar\Omega = 16$ MeV compared with results of Refs. [58, 59].

In our previous works we investigated the role played by spurious center-of-mass states excited by the charge operator and devised a procedure to remove them. We do not repeat the procedure here, but rather refer the reader to Ref. [40] for details. Instead, we present here the result of an analogous analysis of center of mass effects performed on the transverse sum rule. We checked the various contributions of the transverse current operator and found out that, as expected, only the isoscalar electric part suffers from substantial spurious contributions. The difference between a calculation with spurious states and one where those are projected out is shown in Fig. 2. Moreover, this part of the current is an order of magnitude smaller compared to the isovector one. We conclude that the spurious-states contamination plays here a negligible role.

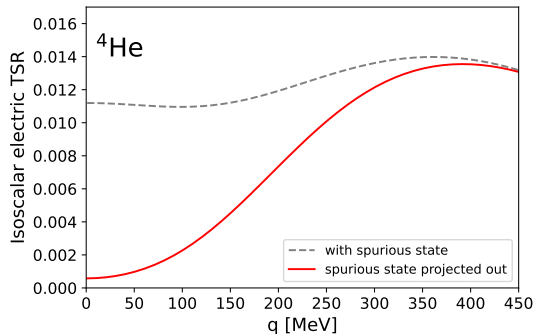


FIG. 2. The effect of spurious states removal in ${}^4\text{He}$ for the isoscalar electric part of the current.

Finally, in Fig. 3 we show the TSR result for ${}^{40}\text{Ca}$ obtained with the NNLO_{sat} potential using the harmonic oscillator frequency $\hbar\Omega = 22$ MeV. Its behaviour is qualitatively similar to ${}^4\text{He}$. We also present separately the electric contribution (shadowed area) which dominates over the magnetic one at lower q . The number of multipoles needed to converge and their relative strength depends on the size of the nucleus and the momentum transfer. In Fig. 4, we show this dependence for four

values of the momentum transfer, $q = 100 - 400$ MeV/c in case of ${}^{40}\text{Ca}$. This information is useful to estimate the numerical cost for calculating the response functions. The number of multipoles needed to get a convergent result grows from four for $q = 100$ MeV/c up to twelve for $q = 400$ MeV/c (for ${}^4\text{He}$ these are three and six, respectively).

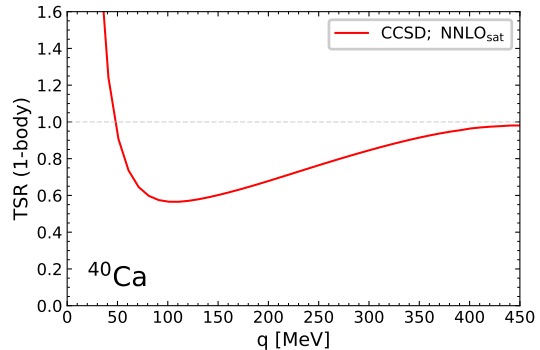


FIG. 3. ${}^{40}\text{Ca}$ results for the transverse sum rule. We employ the NNLO_{sat} , the model space of 15 major oscillator shells and $\hbar\Omega = 22$ MeV. The shadowed region shows the contribution of the electric multipoles only (without the magnetic multipoles).

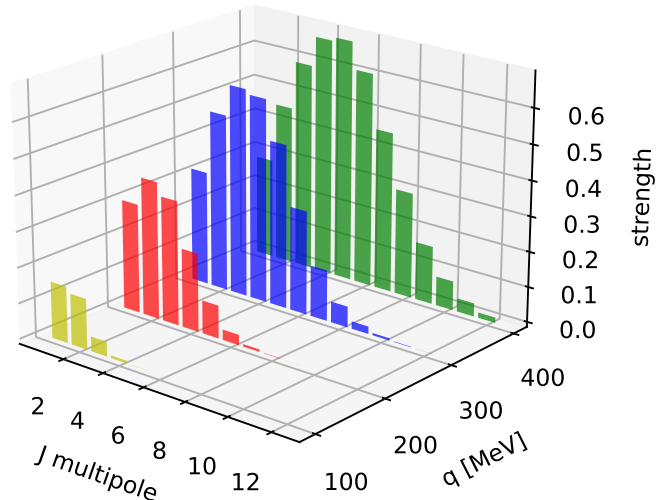


FIG. 4. The strength of various multipoles of the decomposed response as a function of momentum transfer q for ${}^{40}\text{Ca}$.

B. Transverse Response functions

We now turn our attention to the transverse response function, which we calculate from the inversions of the LITs, using an ansatz for the response function. We ex-

pand it in terms of the following basis functions

$$R_T(\omega, q) = \sum_{i=1}^N c_i f_i(\omega; n_0, \beta_i), \quad (12)$$

$$f_i(\omega; n_0, \beta_i) = (\omega - \omega_{th})^{n_0} e^{-\frac{(\omega - \omega_{th})}{\beta_i}}.$$

This form of basis functions is motivated by the threshold behavior of the response function for the deuteron which is known analytically to be $\omega^{\ell+1/2}$ (ℓ is the orbital angular momentum quantum number). The threshold energy ω_{th} is nucleus-dependent and in our case corresponds to the proton separation energy. For various values of σ_I , n_0 and N , we vary the continuous parameter β_i over a wide range. For each combination, we search for the optimal c_i coefficients minimizing the least square fit.

For all the results in this section we performed a robust analysis, varying $n_0 = \{0.5, 1.5\}$, and the number of basis functions $N = \{6, 7, 8\}$. We repeated the simulation for two values of σ_I , namely 5 and 10 MeV. We estimate the inversion uncertainty as the spread between all of the found optimal solutions.

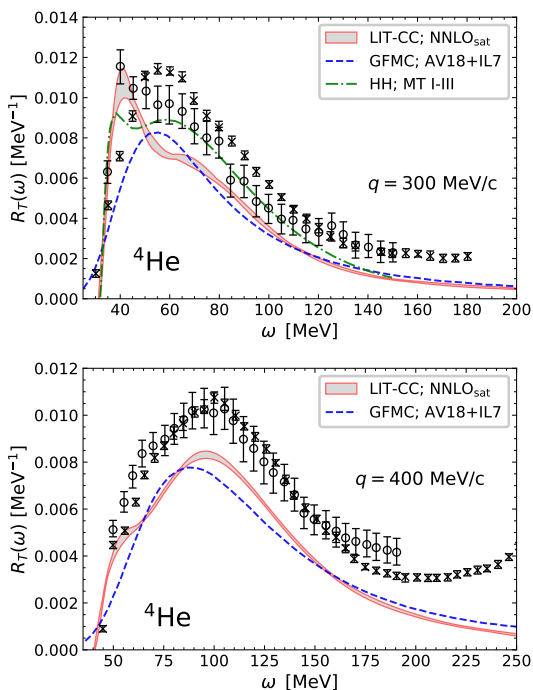


FIG. 5. ${}^4\text{He}$ transverse response function for $q = 300$ and 400 MeV/c using the NNLO_{sat} interaction compared with GFMC predictions using AV18+IL7 potential [60] and hyperspherical harmonics with the MTI-III interaction [61]. Experimental data are taken from Refs. [62] (circles) and [63] (crosses).

In Fig. 5, we present our benchmark results for ${}^4\text{He}$ at the kinematics of $q = 300$ and 400 MeV/c, comparing them with experimental data and other theoretical calculations obtained with one-body currents only. The uncertainty band of our CCSD results comes from the inversion procedure, not from a variation of the harmonic

oscillation frequency, which is kept fixed at $\hbar\omega = 16$ MeV, given that varying it yields negligible differences. The band is a few percent broad and becomes of the order of 10% only in the lower part of the spectrum for $q = 300$ MeV/c. For both considered momentum transfers we observe around 20% missing strength with respect to the experimental data. This fact was already predicted using other nuclear Hamiltonians and many-body methods and was attributed to the lack of two-body currents [34].

We observe, especially for $q = 300$ MeV/c (also visible for $q = 400$ MeV/c), an irregular shape of the quasi-elastic peak. The visible two-peak structure is qualitatively similar to the one obtained from hyperspherical harmonics calculations with the MTI-III potential. For the GFMC result we observe a much smoother quasi-elastic peak with a different low-energy behaviour. We interpret these differences as a result of using (i) different integral transforms: the Lorentz (in our case) or Laplace (for the GFMC), (ii) different nuclear forces, as well as (iii) different inversion procedures. We notice that a similar discrepancy has been already reported for the longitudinal response function in Ref. [60] where the GFMC results were compared with the hyperspherical harmonics using the same interaction but different integral transforms. To get more insight about the shape of the response function, in Fig. 6 we split the contributions to the transverse response function at $q = 300$ MeV/c into the electric/magnetic and isoscalar/isovector parts. This reveals that the low-energy shoulder originates from the magnetic part of current and that the isovector contribution is an order of magnitude larger than the isoscalar.

We proceed to the calculation of the transverse response function for ${}^{40}\text{Ca}$. In this case, we use two different chiral Hamiltonians, employed previously for the longitudinal response function [43], namely the NNLO_{sat} [56] and $\Delta\text{NNLO}_{\text{GO}}(450)$ [57] chiral potentials at next-to-next-to-leading order in a χEFT with and without Δ degrees of freedom, respectively. For the inversion, we use the theoretical values of the proton separation energy, namely $\omega_{th} = 6.9$ MeV for NNLO_{sat} and $\omega_{th} = 8$ MeV for $\Delta\text{NNLO}_{\text{GO}}(450)$, imposing the response function to be zero below this threshold. In our studies of the longitudinal response function we found that the dependence on the $\hbar\Omega$ is negligible when varying it between 16 and 22 MeV. Here, we performed an analogous analysis using $\hbar\Omega = 16$ and 22 MeV and we arrived at the same conclusion for the transverse response function.

Let us briefly comment on the available experimental data for ${}^{40}\text{Ca}$. Two experiments performed the Rosenbluth separation in the past [64, 65] and their results are in tension. In particular, the authors of Ref. [65] found a 25–40% lower Coulomb sum rule. Later, a re-analysis of the world data was performed by Jourdan [66], who presented the results for three values of momentum transfer $q = 300, 380,$ and 570 MeV/c. However, there is not a single value of momentum transfer, for which the data of all of these three analyses is available. Therefore, we

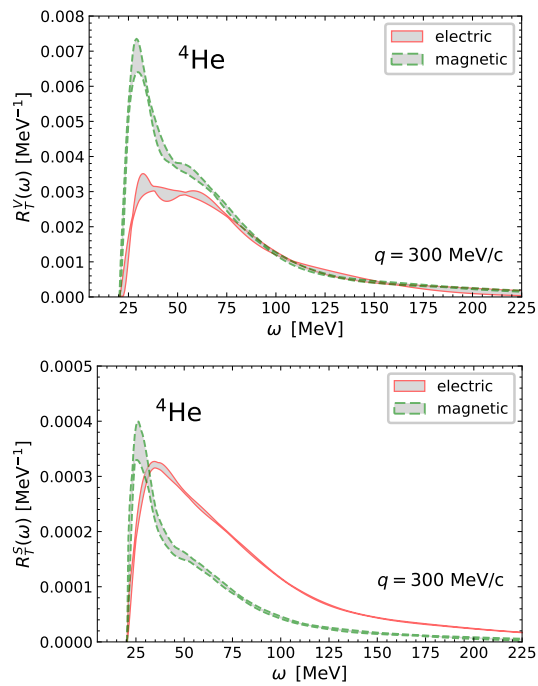


FIG. 6. Response functions on ${}^4\text{He}$ at $q = 300$ MeV/c. The isovector (upper panel) and isoscalar (lower panel) contributions are shown separately for the electric and magnetic part of the transverse current.

decided to show our results at several kinematics against various data-sets.

First we look at $q = 300$ and 380 MeV/c, for which the world data is available. For 300 MeV/c, the re-analysis by Jourdan overlaps to great extent with the original data points from Ref. [64], apart from a few points above 120 MeV. A very good agreement between our calculation and the data for both kinematics is observed, although somehow unexpectedly, since for light nuclei the one-body current gives only 70 – 80% of the strength with respect to the data.

Within our framework we are able to assess several sources of uncertainty, both coming from the chiral expansion of the employed Hamiltonian, as well as from the truncations in the many-body method. To estimate systematic uncertainties from χEFT , we check the response at $q = 300$ MeV/c, for which we used potentials at two orders: $\Delta\text{NLO}_{\text{GO}}(450)$ and $\Delta\text{NNLO}_{\text{GO}}(450)$ of the chiral Hamiltonian (see Fig. 8). The difference between them is at the order of a few percent. This is analogous to our findings for the longitudinal response function [67]. We leave the further studies of the convergence of the many-body method for the future, since it will require much more expensive calculations including triple correlations. However, we can say that first pilot runs including triples excitations do not show any sizable difference in the quasi-elastic peak. It remains to be seen what the effect of two-body currents will be. Work to include them is presently ongoing [68].

Finally, to illustrate the tension between the experiments, in Fig. 9 we show data for $q = 400$ MeV/c [64] and $q = 410$ MeV/c [65] and compare them with our calculations done at $q = 400$ MeV/c, both for the longitudinal and transverse response functions. Experimental data-sets differ even by 30% in the quasielastic peak, although a 10 MeV difference between momentum transfers is not expected to give such a big effect (rather of the order of a few percent). Our results agree considerably better with Ref. [64]. However, the larger prediction of R_T by Ref. [65], would be more consistent with the assumption of large two-body currents contribution.

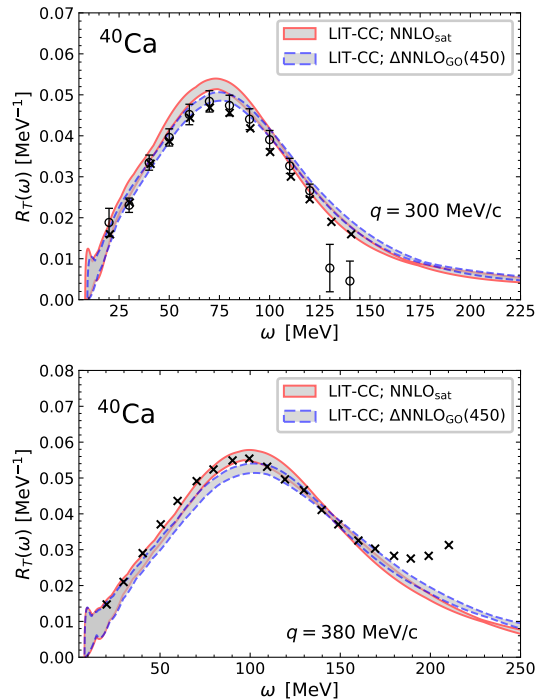


FIG. 7. ${}^{40}\text{Ca}$ transverse response function for $q = 300$ and 380 MeV/c with the NNLO_{sat} and $\Delta\text{NNLO}_{\text{GO}}(450)$ potentials. Experimental data are taken from [64] (circles) and [66] (crosses).

IV. CONCLUSIONS

We presented the first *ab initio* calculation of the transverse response in the region of medium-mass nuclei computed within the LIT-CC method. This work is another step forward in the development of our theoretical program towards calculating electroweak responses for the future neutrino oscillation experiments.

We benchmarked our method on ${}^4\text{He}$ where we found a reasonable agreement with previous calculations and experimental data. Our results underestimate the data, which is expected since we included only one-body current. Nevertheless, the transverse sum rule as a function of q has a very similar behavior as other calculations per-

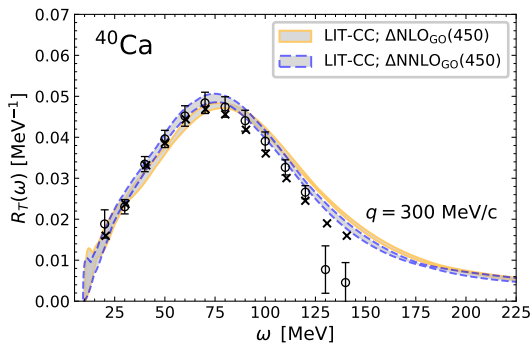


FIG. 8. Dependence of the transverse response function on the chiral order of the Δ -full interaction. Experimental data are taken from [64] (circles) and [66] (crosses).

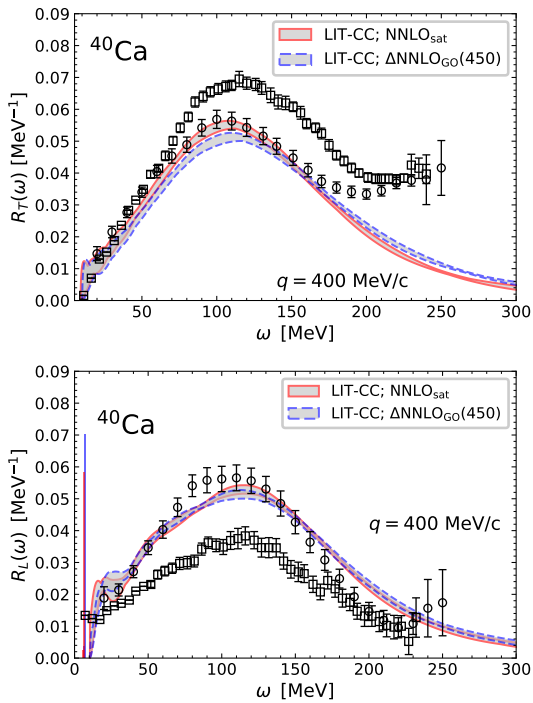


FIG. 9. Transverse and longitudinal response functions for ^{40}Ca calculated for $q = 400$, MeV/c for NNLO_{sat} and $\Delta\text{NNLO}_{\text{G0}}(450)$ potentials. Experimental data for $q = 400$ MeV/c taken from [64] (circles) and for $q = 410$ MeV/c from [65] (squares).

formed with other methods and phenomenological potentials.

Next, we performed an analysis of the transverse response function on ^{40}Ca . Our results stay in a very good agreement with the world data by Jourdan. Our finding motivates further investigations: both the inclusion of the two-body currents, as well as the study of truncations in the many-body expansion are to be performed in the future. We also want to point out that the tension between the ‘two experimental Rosenbluth data on ^{40}Ca have not yet been fully understood and clarified. In view of the long-baseline neutrino programs and of the role electron scattering plays in constraining theoretical predictions, it is important to shed light on this matter. A new experimental program in this direction is being initiated in Mainz [69].

ACKNOWLEDGMENTS

This project has received funding from the European Union’s Horizon 2020 research and innovation programme under the Marie Skłodowska-Curie grant agreement No. 101026014. This work was supported by the Deutsche Forschungsgemeinschaft (DFG) through the Cluster of Excellence ‘‘Precision Physics, Fundamental Interactions, and Structure of Matter’’ (PRISMA⁺ EXC 2118/1) funded by the DFG within the German Excellence Strategy (Project ID 39083149). It is also supported by the U.S. Department of Energy, Office of Science, Office of Nuclear Physics under Award Number DE-SC0018223 (SciDAC-4 NUCLEI) and the SciDAC-5 NUCLEI collaboration, and by the Office of High Energy Physics, U.S. Department of Energy, under Contract No. DE-AC02-07CH11359 through the Neutrino Theory Network Fellowship awarded to BA. Computer time was provided by the supercomputer MogonII at Johannes Gutenberg-Universität Mainz, and by the Innovative and Novel Computational Impact on Theory and Experiment (INCITE) programme. This research used resources of the Oak Ridge Leadership Computing Facility located at Oak Ridge National Laboratory, which is supported by the Office of Science of the Department of Energy under contract No. DE-AC05-00OR22725

- [1] H. Hergert, ‘‘A Guided Tour of *ab initio* Nuclear Many-Body Theory,’’ *Front. in Phys.* **8**, 379 (2020), [arXiv:2008.05061 \[nucl-th\]](#).
- [2] A. Ekström, C. Forssén, G. Hagen, G. R. Jansen, W. Jiang, and T. Papenbrock, ‘‘What is *ab initio* in nuclear theory?’’ *Frontiers in Physics* **11** (2023), [10.3389/fphy.2023.1129094](#).
- [3] Evgeny Epelbaum, Hans-Werner Hammer, and Ulf-G. Meissner, ‘‘Modern Theory of Nuclear Forces,’’ *Rev.*

Mod. Phys. **81**, 1773–1825 (2009), [arXiv:0811.1338 \[nucl-th\]](#).

- [4] A. Gardestig and Daniel R. Phillips, ‘‘How low-energy weak reactions can constrain three-nucleon forces and the neutron-neutron scattering length,’’ *Phys. Rev. Lett.* **96**, 232301 (2006), [arXiv:nucl-th/0603045](#).
- [5] S. Bacca and S. Pastore, ‘‘Electromagnetic reactions on light nuclei,’’ *Journal of Physics G: Nuclear and Particle Physics* **41**, 123002 (2014).

- [6] Baishan Hu *et al.*, “Ab initio predictions link the neutron skin of ^{208}Pb to nuclear forces,” *Nature Phys.* **18**, 1196–1200 (2022), arXiv:2112.01125 [nucl-th].
- [7] M. A. Caprio, P. Maris, J. P. Vary, and R. Smith, “Collective rotation from ab initio theory,” *Int. J. Mod. Phys. E* **24**, 1541002 (2015).
- [8] Kristina D. Launey, Tomas Dytrych, and Jerry P. Draayer, “Symmetry-guided large-scale shell-model theory,” *Progress in Particle and Nuclear Physics* **89**, 101–136 (2016).
- [9] S. J. Novario, G. Hagen, G. R. Jansen, and T. Papenbrock, “Charge radii of exotic neon and magnesium isotopes,” *Phys. Rev. C* **102**, 051303 (2020).
- [10] T. Miyagi, S. R. Stroberg, J. D. Holt, and N. Shimizu, “Ab initio multishell valence-space hamiltonians and the island of inversion,” *Phys. Rev. C* **102**, 034320 (2020).
- [11] Mikael Frosini, Thomas Duguet, Jean-Paul Ebran, Benjamin Bally, Tobias Mongelli, Tomás R. Rodríguez, Robert Roth, and Vittorio Somà, “Multi-reference many-body perturbation theory for nuclei: II. Ab initio study of neon isotopes via PGC and IM-NCSM calculations,” *Eur. Phys. J. A* **58**, 63 (2022), arXiv:2111.00797 [nucl-th].
- [12] G. Hagen, S. J. Novario, Z. H. Sun, T. Papenbrock, G. R. Jansen, J. G. Lietz, T. Duguet, and A. Tichai, “Angular-momentum projection in coupled-cluster theory: Structure of ^{34}Mg ,” *Phys. Rev. C* **105**, 064311 (2022).
- [13] Andreas Ekström, Christian Forssén, G. Hagen, G. R. Jansen, T. Papenbrock, and Z. H. Sun, “How chiral forces shape neutron-rich Ne and Mg nuclei,” arXiv e-prints, arXiv:2305.06955 (2023), arXiv:2305.06955 [nucl-th].
- [14] F. Bonaïti, S. Bacca, and G. Hagen, “Ab initio coupled-cluster calculations of ground and dipole excited states in ^8He ,” *Phys. Rev. C* **105**, 034313 (2022).
- [15] S. Kaufmann, J. Simonis, S. Bacca, J. Billowes, M. L. Bissell, K. Blaum, B. Cheal, R. F. Garcia Ruiz, W. Gins, C. Gorges, G. Hagen, H. Heylen, A. Kanellakopoulos, S. Malbrunot-Ettenauer, M. Miorelli, R. Neugart, G. Neyens, W. Nörtershäuser, R. Sánchez, S. Sailer, A. Schwenk, T. Ratajczyk, L. V. Rodríguez, L. Wehner, C. Wraith, L. Xie, Z. Y. Xu, X. F. Yang, and D. T. Yorandov, “Charge radius of the short-lived ^{68}Ni and correlation with the dipole polarizability,” *Phys. Rev. Lett.* **124**, 132502 (2020).
- [16] F. Coester, “Bound states of a many-particle system,” *Nuclear Physics* **7**, 421 – 424 (1958).
- [17] F. Coester and H. Kümmel, “Short-range correlations in nuclear wave functions,” *Nuclear Physics* **17**, 477 – 485 (1960).
- [18] H. Kümmel, K. H. Lührmann, and J. G. Zabolitzky, “Many-fermion theory in expS- (or coupled cluster) form,” *Physics Reports* **36**, 1 – 63 (1978).
- [19] B. Mihaila and J. H. Heisenberg, “Microscopic Calculation of the Inclusive Electron Scattering Structure Function in ^{16}O ,” *Phys. Rev. Lett.* **84**, 1403–1406 (2000).
- [20] D. J. Dean and M. Hjorth-Jensen, “Coupled-cluster approach to nuclear physics,” *Phys. Rev. C* **69**, 054320 (2004).
- [21] M. Włoch, D. J. Dean, J. R. Gour, M. Hjorth-Jensen, K. Kowalski, T. Papenbrock, and P. Piecuch, “Ab-Initio coupled-cluster study of ^{16}O ,” *Phys. Rev. Lett.* **94**, 212501 (2005).
- [22] G. Hagen, T. Papenbrock, D. J. Dean, and M. Hjorth-Jensen, “Medium-mass nuclei from chiral nucleon-nucleon interactions,” *Phys. Rev. Lett.* **101**, 092502 (2008).
- [23] G. Hagen, T. Papenbrock, D. J. Dean, and M. Hjorth-Jensen, “Ab initio coupled-cluster approach to nuclear structure with modern nucleon-nucleon interactions,” *Phys. Rev. C* **82**, 034330 (2010).
- [24] Sven Binder, Joachim Langhammer, Angelo Calci, and Robert Roth, “Ab initio path to heavy nuclei,” *Phys. Lett. B* **736**, 119 – 123 (2014).
- [25] G. Hagen, T. Papenbrock, M. Hjorth-Jensen, and D. J. Dean, “Coupled-cluster computations of atomic nuclei,” *Rep. Prog. Phys.* **77**, 096302 (2014).
- [26] Calvin W. Johnson *et al.*, “White paper: from bound states to the continuum,” *J. Phys. G* **47**, 123001 (2020), arXiv:1912.00451 [nucl-th].
- [27] Victor D. Efros, Winfred Leidemann, and Giuseppina Orlandini, “Response functions from integral transforms with a lorentz kernel,” *Phys. Lett. B* **338**, 130 – 133 (1994).
- [28] Sonia Bacca, Nir Barnea, Gaute Hagen, Giuseppina Orlandini, and Thomas Papenbrock, “First Principles Description of the Giant Dipole Resonance in ^{16}O ,” *Phys. Rev. Lett.* **111**, 122502 (2013), arXiv:1303.7446 [nucl-th].
- [29] S. Bacca, N. Barnea, G. Hagen, M. Miorelli, G. Orlandini, and T. Papenbrock, “Giant and pigmy dipole resonances in ^4He , $^{16,22}\text{O}$, and ^{40}Ca from chiral nucleon-nucleon interactions,” *Phys. Rev. C* **90**, 064619 (2014), arXiv:1410.2258 [nucl-th].
- [30] M. Miorelli, S. Bacca, N. Barnea, G. Hagen, G. R. Jansen, G. Orlandini, and T. Papenbrock, “Electric dipole polarizability from first principles calculations,” *Phys. Rev. C* **94**, 034317 (2016), arXiv:1604.05381 [nucl-th].
- [31] K. Abe *et al.* (Hyper-Kamiokande Proto-Collaboration), “Physics potential of a long-baseline neutrino oscillation experiment using a J-PARC neutrino beam and Hyper-Kamiokande,” *PTEP* **2015**, 053C02 (2015).
- [32] R. Acciarri *et al.* (DUNE), “Long-Baseline Neutrino Facility (LBNF) and Deep Underground Neutrino Experiment (DUNE),” (2015), arXiv:1512.06148 [physics.ins-det].
- [33] A. Lovato, S. Gandolfi, J. Carlson, Steven C. Pieper, and R. Schiavilla, “Neutral weak current two-body contributions in inclusive scattering from ^{12}C ,” *Phys. Rev. Lett.* **112**, 182502 (2014).
- [34] A. Lovato, S. Gandolfi, J. Carlson, Steven C. Pieper, and R. Schiavilla, “Electromagnetic and neutral-weak response functions of ^4He and ^{12}C ,” *Phys. Rev. C* **91**, 062501 (2015), arXiv:1501.01981 [nucl-th].
- [35] A. Lovato, S. Gandolfi, J. Carlson, Ewing Lusk, Steven C. Pieper, and R. Schiavilla, “Quantum Monte Carlo calculation of neutral-current $\nu - ^{12}\text{C}$ inclusive quasielastic scattering,” *Phys. Rev. C* **97**, 022502 (2018), arXiv:1711.02047 [nucl-th].
- [36] A. Lovato, J. Carlson, S. Gandolfi, N. Rocco, and R. Schiavilla, “Ab initio study of (ν_ℓ, ℓ^-) and $(\bar{\nu}_\ell, \ell^+)$ inclusive scattering in ^{12}C : Confronting the miniboone and t2k ccqe data,” *Phys. Rev. X* **10**, 031068 (2020).
- [37] S. Pastore, J. Carlson, S. Gandolfi, R. Schiavilla, and R. B. Wiringa, “Quasielastic lepton scattering and back-to-back nucleons in the short-time approximation,” *Phys. Rev. C* **101**, 044612 (2020).
- [38] N. Rocco and C. Barbieri, “Inclusive electron-nucleus

- cross section within the Self Consistent Green's Function approach," *Phys. Rev. C* **98**, 025501 (2018), [arXiv:1803.00825 \[nucl-th\]](#).
- [39] C. Barbieri, N. Rocco, and V. Somà, "Lepton scattering from ^{40}Ar and Ti in the quasielastic peak region," (2019), [arXiv:1907.01122 \[nucl-th\]](#).
- [40] J. E. Sobczyk, B. Acharya, S. Bacca, and G. Hagen, "Coulomb sum rule for ^4He and ^{16}O from coupled-cluster theory," *Phys. Rev. C* **102**, 064312 (2020), [arXiv:2009.01761 \[nucl-th\]](#).
- [41] Joanna E. Sobczyk and Sonia Bacca, " ^{16}O spectral function from coupled-cluster theory: applications to lepton-nucleus scattering," (2023), [arXiv:2309.00355 \[nucl-th\]](#).
- [42] M. Khachatryan *et al.* (CLAS, e4v), "Electron-beam energy reconstruction for neutrino oscillation measurements," *Nature* **599**, 565–570 (2021).
- [43] J. E. Sobczyk, B. Acharya, S. Bacca, and G. Hagen, "Ab initio computation of the longitudinal response function in ^{40}Ca ," *Phys. Rev. Lett.* **127**, 072501 (2021), [arXiv:2103.06786 \[nucl-th\]](#).
- [44] A. Lovato, S. Gandolfi, Ralph Butler, J. Carlson, Ewing Lusk, Steven C. Pieper, and R. Schiavilla, "Charge form factor and sum rules of electromagnetic response functions in ^{12}C ," *Phys. Rev. Lett.* **111**, 092501 (2013).
- [45] J.J. Kelly, "Simple parametrization of nucleon form factors," *Phys. Rev. C* **70**, 068202 (2004).
- [46] S. Kolling, E. Epelbaum, H. Krebs, and U. G. Meissner, "Two-pion exchange electromagnetic current in chiral effective field theory using the method of unitary transformation," *Phys. Rev. C* **80**, 045502 (2009), [arXiv:0907.3437 \[nucl-th\]](#).
- [47] Hermann Krebs, "Nuclear Currents in Chiral Effective Field Theory," *Eur. Phys. J. A* **56**, 234 (2020), [arXiv:2008.00974 \[nucl-th\]](#).
- [48] S. Pastore, R. Schiavilla, and J. L. Goity, "Electromagnetic two-body currents of one- and two-pion range," *Phys. Rev. C* **78**, 064002 (2008), [arXiv:0810.1941 \[nucl-th\]](#).
- [49] Bijaya Acharya and Sonia Bacca, "Gaussian process error modeling for chiral effective-field-theory calculations of $\text{np} \leftrightarrow \text{d} \gamma$ at low energies," *Phys. Lett. B* **827**, 137011 (2022), [arXiv:2109.13972 \[nucl-th\]](#).
- [50] V D Efros, W Leidemann, G Orlandini, and N Barnea, "The lorentz integral transform (lit) method and its applications to perturbation-induced reactions," *Journal of Physics G: Nuclear and Particle Physics* **34**, R459 (2007).
- [51] I. Shavitt and R. J. Bartlett, *Many-body Methods in Chemistry and Physics* (Cambridge University Press, Cambridge UK, 2009).
- [52] R. J. Bartlett and M. Musiał, "Coupled-cluster theory in quantum chemistry," *Rev. Mod. Phys.* **79**, 291–352 (2007).
- [53] S. Bacca, N. Barnea, G. Hagen, G. Orlandini, and T. Papenbrock, "First principles description of the giant dipole resonance in ^{16}O ," *Phys. Rev. Lett.* **111**, 122502 (2013).
- [54] John F. Stanton and Rodney J. Bartlett, "The equation of motion coupled-cluster method. a systematic biorthogonal approach to molecular excitation energies, transition probabilities, and excited state properties," *J. Chem. Phys.* **98**, 7029–7039 (1993).
- [55] Sonia Bacca, Hartmuth Arenhövel, Nir Barnea, Winfried Leidemann, and Giuseppina Orlandini, "Inclusive electron scattering off ^4He ," *Phys. Rev. C* **76**, 014003 (2007).
- [56] A. Ekström, G. R. Jansen, K. A. Wendt, G. Hagen, T. Papenbrock, B. D. Carlsson, C. Forssén, M. Hjorth-Jensen, P. Navrátil, and W. Nazarewicz, "Accurate nuclear radii and binding energies from a chiral interaction," *Phys. Rev. C* **91**, 051301 (2015), [arXiv:1502.04682 \[nucl-th\]](#).
- [57] W. G. Jiang, A. Ekström, C. Forssén, G. Hagen, G. R. Jansen, and T. Papenbrock, "Accurate bulk properties of nuclei from $a = 2$ to ∞ from potentials with Δ isobars," *Phys. Rev. C* **102**, 054301 (2020).
- [58] R. Schiavilla, "Sum Rules of the Transverse Response Functions of $a = 2, 3$ and 4 Nuclei," *Nucl. Phys. A* **499**, 301–327 (1989).
- [59] J. Carlson, J. Jourdan, R. Schiavilla, and I. Sick, "Longitudinal and transverse quasielastic response functions of light nuclei," *Phys. Rev. C* **65**, 024002 (2002), [arXiv:nucl-th/0106047](#).
- [60] Noemi Rocco, Winfried Leidemann, Alessandro Lovato, and Giuseppina Orlandini, "Relativistic effects in ab-initio electron-nucleus scattering," *Phys. Rev. C* **97**, 055501 (2018), [arXiv:1801.07111 \[nucl-th\]](#).
- [61] S. Bacca, H. Arenhoevel, N. Barnea, W. Leidemann, and G. Orlandini, "Inclusive electron scattering off He-4," *Phys. Rev. C* **76**, 014003 (2007), [arXiv:nucl-th/0612009](#).
- [62] S. A. Dytman, A. M. Bernstein, K. I. Blomqvist, T. J. Pavel, B. P. Quinn, R. Altemus, J. S. Mccarthy, G. H. Mechtel, T. S. Ueng, and R. R. Whitney, "Inclusive Electron Scattering From ^2H , ^3He , and ^4He ," *Phys. Rev. C* **38**, 800–812 (1988).
- [63] A. Zghiche *et al.*, "Longitudinal and transverse responses in quasielastic electron scattering from ^{208}Pb and ^4He ," *Nucl. Phys. A* **572**, 513–559 (1994), [Erratum: *Nucl.Phys.A* 584, 757–757 (1995)].
- [64] C. F. Williamson *et al.*, "Quasielastic electron scattering from Ca-40," *Phys. Rev. C* **56**, 3152–3172 (1997).
- [65] Z. E. Meziani *et al.*, "Coulomb Sum Rule for Ca-40, Ca-48, and Fe-56 for $-\text{q}$ (Vector) $\leq 550\text{-MeV}/c$," *Phys. Rev. Lett.* **52**, 2130–2133 (1984).
- [66] J. Jourdan, "Quasielastic response functions: The Coulomb sum revisited," *Nucl. Phys. A* **603**, 117–160 (1996).
- [67] Bijaya Acharya, Sonia Bacca, Francesca Bonaiti, Simone Salvatore Li Muli, and Joanna E. Sobczyk, "Uncertainty quantification in electromagnetic observables of nuclei," (2022), [arXiv:2210.04632 \[nucl-th\]](#).
- [68] B. Acharya *et al.*, in preparation.
- [69] L. Doria and M. Mihovilovic, private communication.